CHAPTER 1

Introduction and Scope of the Thesis

Contents

CHAPTER 1

Introduction and Scope of the Thesis

1.1 Introduction

Sensors are the devices that generate a useful signal related to the quantity measured [Bolton, (1999)]. It is defined by the Instrument Society of America as "*A device which provides a usable output in response to a specified measurand*". Nowadays, electronic sensors are widely used in automation work and sophisticated instrumentation [National Academies Press; 1995]. The very first electric/electronic sensor was developed by Wilhelm von Siemens for the detection of temperature change using a copper resistor in 1860 [National Academies Press; 1995]. Till date, several types of sensors like temperature sensors, light sensors, pressure sensors, touch sensors, colour sensors, proximity sensors, accelerometer sensors, infrared sensors, ultrasonic sensors, flow and level sensors, humidity sensors, smoke sensors, gas sensors, alcohol sensors, etc. have been developed by the researchers [Internet resource (IR1)] for various applications in our modern day's life activities. Most of the modern day's sensors are compatible with the large-scale CMOS chips to convert physical phenomena into measurable electrical output readily accessible by a digital computer [National Academies Press; 1995]. Recent research in nanomaterials has enabled us to achieve better control of sensing parameters with cutting-edge features, greater fidelity, enhanced reliability, and lower-cost over the bulk materials-based sensors [National Academies Press; 1995].

Human beings are blessed with many naturally powerful sensors in the form of eyes, ears, nose, tongue, and skin to sense light, sound, smell, taste, and heat, respectively. The workings of these natural sensors are very much complex and hence are difficult to emulate them artificially [Balaguru and Jeyaprakash (2004)]. However, the relentless efforts of the scientists and researchers have enabled us to develop many efficient electronic sensors to measure and quantify various physical quantities. The electronic noses which can sense and quantify the presence of various harmful gases are known as *gas sensors*.

Metal oxide nanomaterials have been widely explored for developing various modern gas sensors. The working of gas sensors is primarily based on the physical and chemical interaction with analyte species through adsorption, chemical reaction, or charge transfer. The interaction provides the change in the physicochemical properties of the nanomaterials, namely their temperature, mass, and electrical resistance [Balaguru and Jeyaprakash (2004)]. In the early days of the mining industries, Canaries (birds) in small cages and then Flame Safety Lamp (Davey's Lamp) were used for the detection of poisonous gases inside the mines [Burrell (1914), Balaguru and Jeyaprakash (2004)]. A real breakthrough in the area of gas detection came in 1953 when Walter Brattain and John Bardeen first reported the gas sensing effects on the germanium semiconductor [Brattain and Bardeen (1953)]. Later, a revolution in research and development of gas sensors was started with the study of sensing effects on metal oxide materials by Naoyoshi Taguchi in 1968 [Balaguru and Jeyaprakash (2004)]. He had established the company Figaro Engineering in 1969 to commercialise the metal oxide semiconductors-based sensors [Internet resource (IR2), Balaguru and Jeyaprakash 2004]. Since metal oxide nanostructures are the most widely used materials for modern days gas sensors,

the present thesis reports some metal oxide nanostructure-based gas sensors for the detection of hydrogen gases.

Hydrogen is a highly flammable gas and widely used in the oil refinery/reactant, hydrogenation for sulfur separation, as a coolant in power plant for an electrical generator, fertilizer industry for generation of ammonia, space flight as propulsion fuel, epitaxial growth of silicon from silicon tetrachloride [M. Kumar *et al.* (2017)]. Also, hydrogen is taken as an alternative energy source to counter the limited stock of fossil fuels [Choi *et al* (2017)]. Hydrogen provides clean and pollution-free combustion for energy generation [Zhang *et al.* (2016), Lu *et al.* (2019), Jarwal *et al.* (2019)]. However, hydrogen has some critical issues, namely highly explosive (>4%) and low ignition energy (0.02 mJ), so that its production, transportation, and storage need high safety precautions [Huang *et al.* (2010), Ling *et al.* (2014), Luo *et al.* (2017)]. In this point of view, there is a need for highly selective and susceptible hydrogen gas sensors at low cost and low consumption of power for the detection of any leakage of hydrogen in the industries or domestic sectors [Wang *et al.* (2012), Haija *et al.* (2016), Ranjan et al. (2017), Lee *et al.* (2018), Pour *et al.* (2018)]. Additionally, hydrogen gas has a reducing nature, which promotes reduction when interacted with any materials. Thus, the sophisticated and fast response hydrogen sensors are fabricated and implemented based on this reducing property of hydrogen gas [Yadava *et al.* (1990), Dwivedi *et al.* (1998)].

1.2 Sensing Materials and Working Mechanism for Hydrogen Sensor

The hydrogen sensor based on thin-film electronic devices has drawn large attention due to low fabrication cost. Thin-film electronic devices are made by utilizing the electrical conductivity of the materials, namely conductor, semiconductor, and insulator [Trung, and Lee (2017)]. The electronic or conducting properties of these

materials are altered when interacted with the physical quantity such as temperature, humidity, gases, etc. The interaction with gases results in the physiochemical changes in the materials, which subsequently alter the electronic conductivity. The change in the electronic conductivity also depends significantly on the device and material structure [Arshak *et al.* (2004)]. It is found that the large exposure area in the thin film device results in a bigger change in the electronic conductivity, thus higher gas response or sensitivity. Commonly, Schottky diode [Hunter *et al.* (1997)], PN diode [Juang (2019)], metal-semiconductor-metal (MSM)[C. Kumar *et al.* (2018)], metal-insulator-semiconductor (MIS) capacitor [Lee *et al.* (2011)], metal-oxide-semiconductor (MOS) capacitor [Lu *et al.* (2007)], and thin-film transistor [C. Kumar *et al.* (2018)] are used for the thin film-based gas sensor device structure.

The main part of the thin film gas sensors device is sensing materials, whose conductivity is changed when interacting with the specific gases. A large number of materials such as silicon, germanium, metal oxides (ZnO, TiO_2, SnO_2, etc.), polymers (P3HT, PQT-12, PBTTT, etc.), graphene, etc. have shown the promising gas response for the specific gases [G. Neri (2015)]. Among these materials, metal oxides are widely investigated for gas sensing applications, especially hydrogen. Metal oxides represent a heterogeneous class of materials whose chemical, physical, electrical/electronic, optical, and magnetic properties are found ranging from metals to semiconductors to insulators [Gas'kov and Rumyantseva 2001].

1.2.1 Metal Oxides for Hydrogen Sensors

The semiconductor properties, structural simplicity, and low cost of metal oxides are the key features for their applications in hydrogen sensing. The electrical conductivity of the metal oxide changes greatly under the influence of hydrogen gas

around the surface [Balaguru and Jeyaprakash (2004)]. The increase/decrease in the conductivity after interacting with the reducing hydrogen gas depends on the dominant charge carrier type (electron or hole) in the material (n-type or p-type). In "n-type" semiconductors (TiO_2, ZnO, SnO_2, etc.), conductivity increases whereas conductivity decrease in p-type semiconductors (CuO, Cr_2O_3, etc.) due to interaction with hydrogen gas [Balaguru and Jeyaprakash (2004), Bârsan (2011)].

Based on the electronic structure, metal oxide semiconductors are divided into the following categories [Balaguru and Jeyaprakash (2004)].

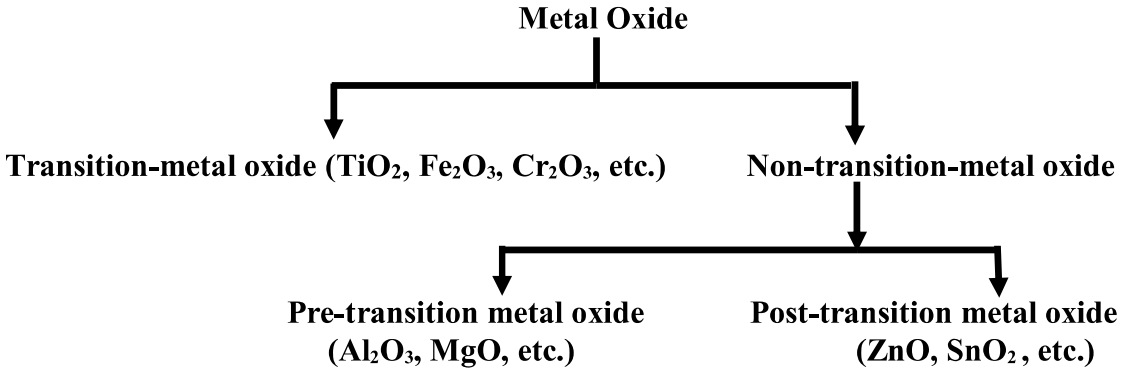

Pre-transition metal oxides are generally inert towards the gases due to the large bandgap, so rarely implemented in gas sensing applications. Post-transition metal oxides are relatively much sensitive to various gases than pre-transition-metal oxides, but their application is limited due to structural instability and non-optimality for the low-temperature operation of the gas sensor [Balaguru and Jeyaprakash (2004)]. Therefore, the transition and post-transition metal oxides with respective electronic configurations of d^0 and d^{10} are most suitable for low-temperature gas sensing applications [Balaguru and Jeyaprakash (2004)]. Most widely used metal-oxide semiconductor-based hydrogen sensors are made up of metal-oxide such as stannic oxide (SnO_2) [Zhao *et al.* (2011)], titanium dioxide (TiO_2) [Zhang *et al.* (2016)], zinc oxide (ZnO) [Mondal *et al.* (2014)], tungsten trioxide (WO_3) [Zhang *et al.* (2013)],

niobium pentoxide (Nb_2O_5) [Wang *et al.* (2012)], etc. The d^0 electronic configuration is mainly exhibited by binary transition metal oxides, namely V_2O_5, TiO_2, etc., whereas the d^{10} configuration is exhibited primarily by post-transition-metal oxides, namely SnO_2, ZnO, etc.

1.2.1.1 Role of TiO_2 in Hydrogen Gas Sensing

TiO_2 has d^0 electronic configuration state available due to which it exhibits Ti^{3+} and Ti^{2+} oxidation state. TiO_2 shows polymorphism properties having many crystalline structures, including rutile (*tetragonal*), anatase (*tetragonal*), and brookite (*orthorhombic*). The structure of the unit cell of each crystalline structure is shown in Figure 1.1. The Grey color represents the Ti atom and the red color represents the O atom.

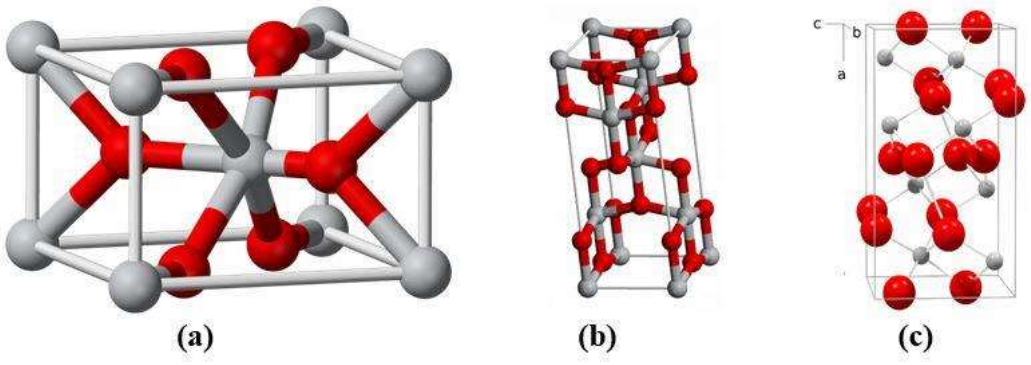

Figure 1.1: Unit cell of the structures (a) rutile (b) anatase, and (c) brookite [IR3]

The basic shape of the anatase is octahedrons with the shared edge to neighbor. On the other hand, rutile and brookite have octahedrons shape but shared both vertex and edge. The bandgap for rutile structure is ~3.0 eV, whereas ~3.4 eV and ~3.3 eV for anatase and brookite structure respectively [Pascual *et al.* (1978), Amtout, and Leonelli (1995), Tang *et al.* (1995), Mattssom, and Osterlund (2010)]. For gas sensing application, surface defects (O ion vacancies) in the material (created by ion or electron bombardment) are necessary because it modulates the material's electronic structure

[Eranna *et al*. (2004)]. Rutile structure is a widely used material for gas sensing applications due to its stable phase [Sharma *et al*. (1997)]. Additionally, nanocrystalline thin films of TiO_2, composite with different metals, and layered structure with catalytic noble metals (i.e., Pt and Pd) increase the chemisorption of hydrogen due to enhanced electron capturing by oxygen ions in the metal oxides [Eranna *et al*. (2004)].

1.2.1.2 Role of ZnO in Hydrogen Gas Sensing

ZnO has two common crystalline structures (like TiO_2), namely wurtzite *(hexagonal)* and zinc blende *(tetrahedral)*. The unit cell of each crystalline structure is shown in Figure 1.2. The green color shows the Zn atom and the blue color shows the O atom.

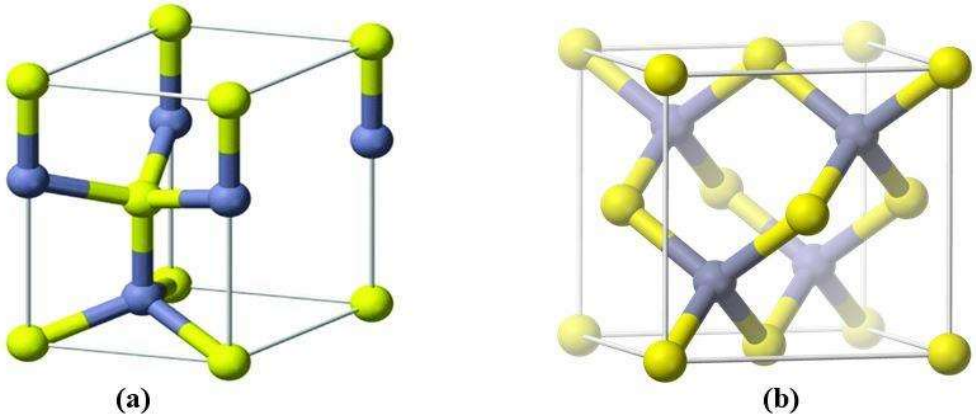

Figure 1.2: Unit cell of the structures (a) Wurtzite and (b) Zinc blend [IR4]

Wurtzite structured ZnO has lower ground-state energy [Arya *et al*. (2012)] and widely used as a sensing layer for reducing gases, namely H_2, CH_4, CO [Srikant, and Clarke (1998)] as well as various volatile organic compounds (VOCs) [Bagheri *et al*. (2014), Zhang *et al*. (2017)]. Moreover, heating at high temperature creates point defects on the ZnO surface, which results in increased charge transfer rate and band bending due to gas adsorption, responsible for promising gas sensing characteristics

[Henrich, and Cox (1994)]. However, it is possible to bring down the operating temperature in the range of 127 to 200 ^{0}C, by adding certain impurities or making nanostructures such as QDs, nanorods, tetrapods, nanowires, nanohelices, etc. [Eranna *et al.* (2004)]. It is also possible to increase the sensitivity towards the specific gas by doping with single or two different noble metals [Tamaekong *et al.* (2009), Fan *et al.* (2017)]. Low gas response and lack of selectivity are the main problems with ZnO based sensor operated at room temperature.

1.2.2 Nanostructured Materials for Hydrogen Sensor

In 1959, Richard Feynman had described how the physical properties could be changed after scaling things at small scales [Internet resource (IR5)]. He had discussed the benefits of manipulating and controlling things on a small scale. According to quantum mechanical theory, carrier confinements could happen in structural elements (i.e., clusters, crystallites, or molecules) of the nanomaterials (NMs) in the range of 1 to 100 nm [Sze (1981), Paul and Giri, (2017)]. Based on the number of dimensions in the nanoscale regime, there are four common types of the NMs, namely three-dimensional (3D), two-dimensional (2D), one dimensional (1D), and, zero-dimensional (0D) as shown in Figure 1.3 [Sudha *et al.* (2018)]. Table 1.1 illustrates the various dimensions of NMs. The unique advantages of nanomaterial (NMs) are widely utilized in the most flourishing areas of scientific research in the thin-film based devices for various electronic, optoelectronic, and sensing applications [Jariwala *et al.* (2013)]. Moreover, quantum dots (0D) of the metal oxides and nanostructures noble metals have shown promising performance for the specific requirement of higher gas response, fast response-recovery time, and high selectivity due to increased surface to volume ratio.

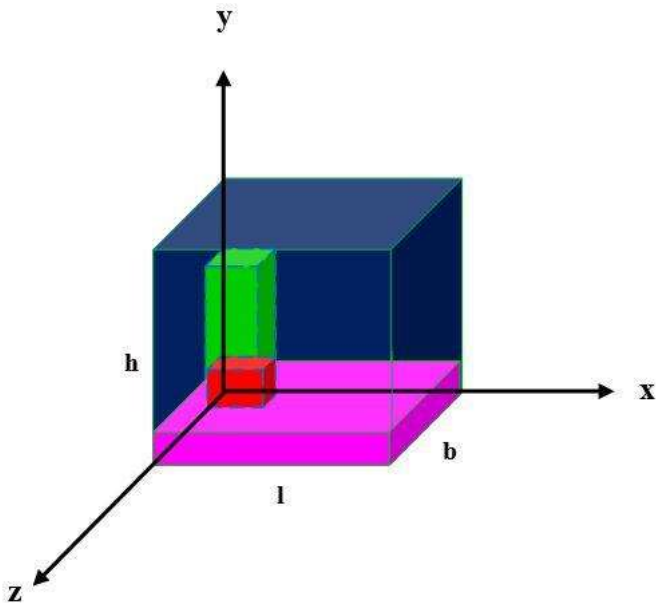

Figure 1.3: Types of NMs based on the number of dimensions in the nanoscale regime.

Table 1.1: Comparison of the various dimensions of NMs.

Types of the NMs	Dimensions	Example
0D	**All the dimensions (l,b,h) at the nanoscale (<100 nm).**	Quantum dots (QDs), Clusters, etc.
1D	**Two dimensions (l,b) at the nanoscales, and one dimension (h) at the microscale.**	Nanotubes, Nanorods, Nanowires, Nanofilament, and Nanofibers, etc.
2D	**One dimension (h) at the nanoscale, and two dimensions (l,b) at the microscale.**	Nano-films, Nano-coatings, Nano-layers, Nano-tapes, Nano-sheets, etc.
3D	**No dimensions at the nanoscale, all dimensions (l,b,h) at the microscale.**	Polycrystals, Nano-particles, Nano-flowers, Nano-pores, etc.

1.2.2.1 Quantum Dots

Quantum confinement effect or quantum size effect [Klimov (2010)] phenomena says that if the size of the semiconducting material is maintained below exciton Bohr radius (mostly below 10 nm), the bandgap of the semiconducting materials can be tuned significantly. The nanoparticles which follow the aforementioned properties are called quantum dots (QDs). Depending on the size, composition, and structure, QDs are divided into three groups, namely, core-type QDs, core-shell QDs, and alloyed QDs [Yoffe *et al*. (2001)].

Core-type QDs: These QDs are composed of single compound materials, typically a metal oxide, metallic chalcogenide, etc., with uniform internal compositions, e.g., ZnO, cadmium telluride (CdTe), lead sulfide (PbS), etc. The electronic, optical, and sensing properties are tuned by changing the size of crystallite of core-type QDs.

Core-shell QDs: These type of QDs consists of a core-type material and a surrounding shell of another material with a higher bandgap [Smith *et al*. (2009)]. The efficiency of core-shell QDs is significantly better than the core-type QDs. An example of core-shell QDs is cadmium selenide-zinc sulfide (CdSe-ZnS) QDs. Here, CdSe is the core and ZnS is the shell.

Alloyed QDs: Alloyed QDs are composed of multiple materials but in a homogeneous mixture rather than a distinct region. Alloyed semiconductors QDs are formed by allowing two semiconductors of different bandgap energy imparts new distinct properties to the particles that are distinct from the original material, e.g., alloyed QDs of the composition CdS_xSe_{1-x}/ZnS of 6 nm diameter emits light of different wavelength by just changing the composition [Vastola *et al*. (2012)].

1.2.2.2 Nanostructured Noble Metals

The catalytic property of noble metals encourages the disintegration of target gas into active radicals; subsequently, improve the reaction rate [Tomer *et al.* (2019)]. Moreover, the nanostructure noble metals have shown unique properties of relatively fast gas molecule disintegration at the surface. Thus, the disintegration of gas molecules results in further improved gas sensitivity. Pd, Pt, Au, and Ag are the generally used noble metals for enhancing the sensitivity of gas sensor [Zhou *et al.* (2014)]. The nanostructure noble metal also produces an active site on the semiconductor's surface, which increases the adsorption of target gas and increases its concentration at the surface [Takeguchi *et al.* (2001), Keane *et al.* (2003), Adams *et al.* (2010)]. The lower Fermi level of noble metal than the semiconductors material used for gas sensing provides movement of the electron from semiconductors into noble metal. As a result, noble metal gets negatively charged, and semiconductors become positively charged, and finally, the semiconductor's energy band is bent at the interface, and a Schottky barrier is formed. Thus, the recombination of electron-hole is prevented, which increases the response to target gas [Lueking *et al.* (2002), Annanouch *et al.* (2016), Boudjahem *et al.* (2017)].

1.2.3 Working Mechanism of Hydrogen Sensor

Gas sensing phenomena in the electronic device based sensor depends on many factors, including the materials, surface morphology, device structure, and operating temperature [Yadava *et al.* (1990), Balaguru and Jeyaprakash (2004), Adams *et al.* (2010)]. The gas response of the metal oxide-based sensors primarily depends on the change in the following parameters:

(i) Conductance

(ii) Dielectric constant

(iii) Mass of the sensing element due to adsorption of gases

(iv) Work function

The presence of target gases at the surface of the sensor changes any of these quantities. The gas sensors' important parameters are gas response (or sensitivity), detection limit, response time, recovery time, and selectivity. These parameters are affected by many factors, including materials, surface morphology, device structure, gas concentration, and operating condition [Balaguru and Jeyaprakash (2004)]. The sensing mechanism in metal oxide-based gas sensors is different at room temperature and higher temperature, as discussed in the following section.

1.2.3.1 Room Temperature Based Hydrogen Sensor

Most of the metal oxide-based gas sensors are insensitive or relatively less sensitive to the target gases when operated at room temperature. After the physical or chemical adsorption of analyte gases, the charge carriers cannot be sufficiently excited to change electrical parameters. However, some nanostructures, such as quantum dots, nanorods, nanofibers, etc., have shown a significant change in electrical parameters due to excitation of the ground-state electron at room temperature [Luo *et al.* (2017)]. Nanostructures also enhance the surface-to-volume ratio, as illustrated in Figure 1.4, and the dangling bonds on the nanostructure surface which increase the adsorption of the target gases and enhance the sensitivity [Luo *et al.* (2017)].

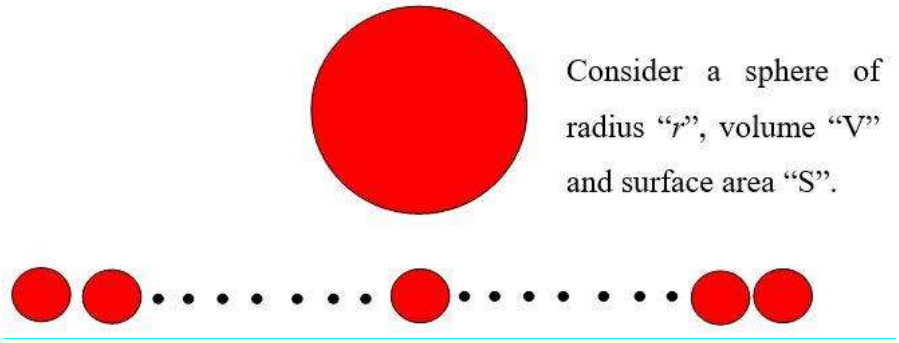

The large sphere is converted into 1000 equal volume spheres with radius: $r_1 = \frac{r}{10}$

The volume of each small sphere: $V_1 = \frac{4}{3}\pi r_1^3 = \frac{V}{1000}$

Surface Area of each unit: $S_1 = 4\pi\left(\frac{r}{10}\right)^2 = \frac{S}{100}$

Total Surface Area: $S_{eff} = 1000S_1 = 10S$.

Figure 1.4: Illustration of the effective surface to volume ratio in nanostructure materials. The surface area to volume ratio is increased by 10 times in the illustrated condition.

1.2.3.2 Temperature Based Hydrogen Sensor

The high-temperature operation of metal oxide-based gas sensors improves gas response, selectivity, and response/recovery time. The gas sensing process at higher temperature is controlled by the electron capturing by oxygen ions (O^-_2, O^-, O^{2-}). The following reaction mechanisms take place for the formation of oxygen ions under the gas adsorption at high temperature [Zhang *et al*. (2016)]:

$$O_2(gas) \longrightarrow O_2(ads) \quad (1.1)$$

$$O_2(ads) + e^- \longrightarrow O^-_2 \quad (1.2)$$

$$O_2(ads) + 2e^- \longrightarrow 2O^- \quad (1.3)$$

$$O_2(ads) + 4e^- \longrightarrow 2O^{2-} \quad (1.4)$$

Since hydrogen is a reducing gas, the hydrogen molecule tries to lower the metal oxide's work function. When H_2 gas is exposed to metal oxide's surface, an electron is shifted from gas molecules to the metal oxide's surface and creates H^+ ions. Thus, the concentration of surface electron increases in n-type metal oxides, like ZnO, TiO_2, and SnO_2, which decreases the resistance. On the other hand, the concentration of holes decreases in p-type metal oxide, like CuO, Cr_2O_3, which increases the resistance [Choi *et al.* (2010), Xiao *et al.* (2015), Bagal *et al.* (2015)]. During the interaction, the adsorbed electron is transferred into the oxygen ions and finally shifted to the metal oxide, which is accounted for the change in the resistance [Boudiba *et al.* (2013)]. Sensitivity is evaluated by measuring the change in resistance under gas exposure.

1.3 Fabrication Techniques for Thin Film Devices

The thin-film (TFs) deposition technique is a process of applying a thin layer upon another surface or substrate. The deposition techniques allow to control the thickness of the layer from a few nanometers to a few micrometers, and some techniques allow single layers of the atom. The deposition technique and the environment under which deposition is performed strongly affect the structural, chemical, optical, electrical properties of the semiconductor nanostructured thin film deposited on the desired substrate [Alferov (2001), Chen, and Mao (2007), Paul, and Giri (2017)]. It is observed that the properties of TFs of material on the desired substrate by using two different deposition techniques are totally different from each other. Even though the same deposition method but under different growth conditions, different TFs are obtained. Thus, the same deposition technique and identical growth conditions are required to be maintained each time for achieving repeatability in the characteristics of nanoelectronic devices. Metal oxide-based large-area gas sensors are fabricated by using several

physical and chemical deposition techniques, namely sputtering, electron beam evaporation, thermal evaporation, hydrothermal, spin-coating, etc. [Yao *et al.* (2008), Dey *et al.* (2017)]. Thermal, electron beam evaporation, and spin-coating briefly discussed in the following subsection are used in the present thesis work.

1.3.1 Thermal Evaporation

It is the simplest deposition technique used for TF deposition. In this technique, atoms and clusters of atoms or molecules of the target material are evaporated in the form of vapor flux from a heating element by passing a current through it. Typically heating elements are made up of carbon, molybdenum, tungsten, and composite ceramic [Martín-Palma, and Lakhtakia (2013)]. The thermal evaporation technique mainly depends on two parameters: the melting point of the material and the effective vacuum level inside the chamber [Jilani *et al.* (2017)]. The general schematic diagram of the thermal evaporation technique is illustrated in Figure 1.5.

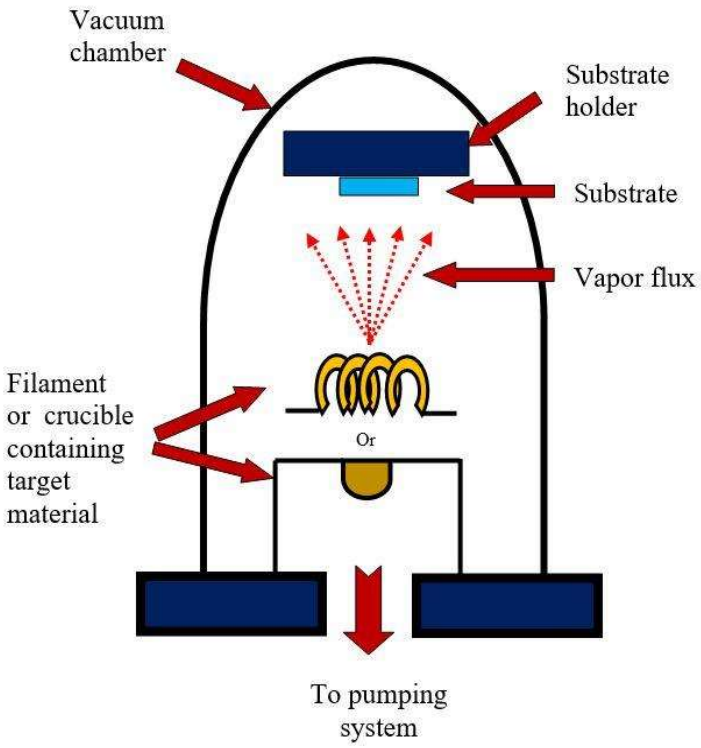

Figure 1.5: General schematic diagram of thermal evaporation

High deposition rates, relatively simple, and cost-effectiveness of the equipment are the major advantage of the thermal evaporation technique. But the technique is not much suitable for fabricating composites/multi-components based TF because of the difference in the melting temperature.

1.3.2 Electron Beam Evaporation

The electron beam evaporation (EBE) technique has a different mechanism for heating the evaporating materials. A filament is used to generate the intensive beam of high energy electrons typically accelerated with voltages from 5 to 20 kV, and this electron beam is focused on the material placed inside a crucible in the EBE. Enough heat is generated due to high energy electrons' bombardment, which evaporates the materials having very high melting points under a high vacuum environment. Crucibles are generally made using graphite, boron nitride, molybdenum, tungsten, etc., depending on the target materials [Martín-Palma, and Lakhtakia (2013)]. The basic configuration of the EBE unit, including heater, electron beam source, substrate holder, top cover, thickness monitor, etc., is shown in Figure. 1.6. The evaporated particles travel towards the cold substrate to get condensed in the form of a TF. Usually, a high vacuum in the range of $\sim 10^{-6} - 10^{-5}$ mbar is maintained in the deposition unit to prevent any type of chemical reaction between the evaporating material/thin-film and background gases. EBE technique offers superb material utilization and low contamination for developing high-quality TFs of different materials along with controlling the film thickness and deposition rate [Huang *et al.* (2011), Vishwas *et al.* (2012), Shougaijam *et al.* (2016), Lokhande *et al.* (2016)].

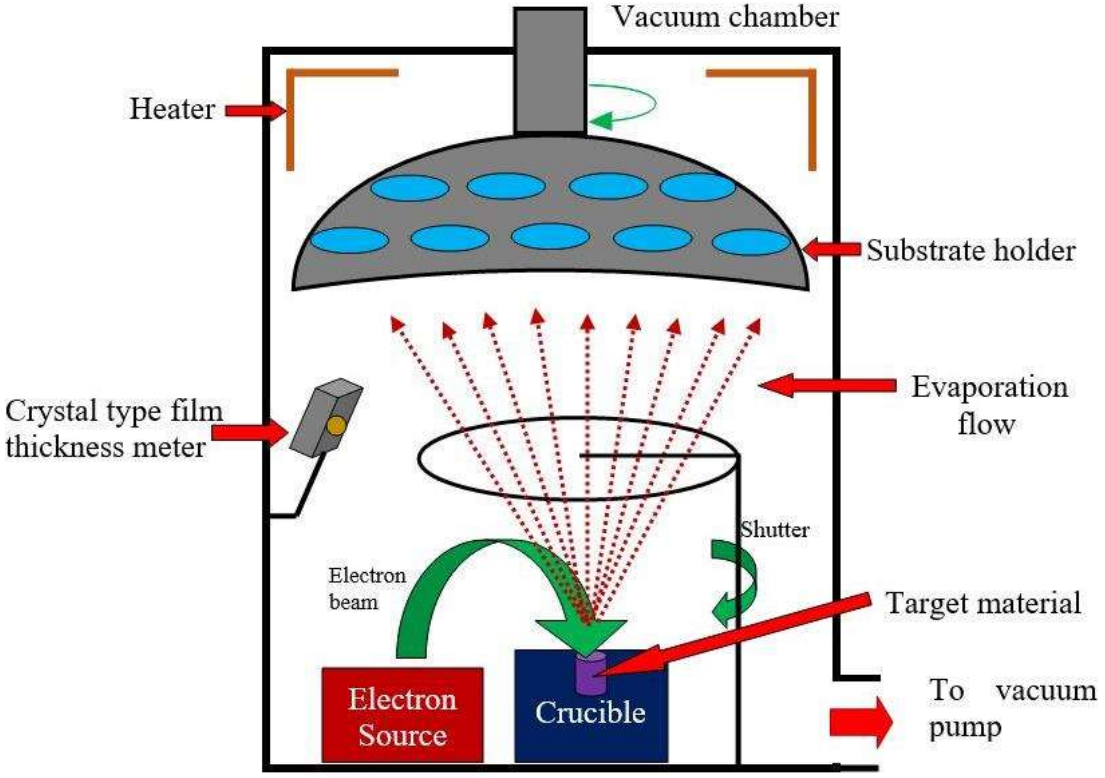

Figure 1.6: Schematic diagram of electron beam evaporation.

1.3.3 Spin Coating

The spin-coating technique is a well-established, low-cost solution-based process to deposit uniform TFs on a flat substrate. Centrifugal force is applied for the uniform spreading of the drop-casted solution on the sample. The thickness and quality of the obtained TFs depend on the solution concentration, viscosity of the solution, and surface tension along with rotation speed, acceleration, and time [Mishra *et al*. (2019)]. Figure 1.7 shows the different stages followed in the spin-coating method.

The solution required for the spreading over the sample is prepared by either dissolving in an appropriate solvent or synthesizing using the "Sol-gel" technique. Sol-gel is a synthesis process involving conversion from solution to gel before deposition [Thomas (1993)]. It is a wet chemical process commonly used for metal oxide synthesis [Chen and Mao (2007)]. In this process, a metal alkoxide (precursor), is dissolved in an

appropriate solvent, and then a suitable catalyst is added to enhance the rate of reaction. Afterward, the precursor forms M-O-M bonds by undertaking hydrolysis and polycondensation processes. Figure 1.8 illustrates the Sol-gel process.

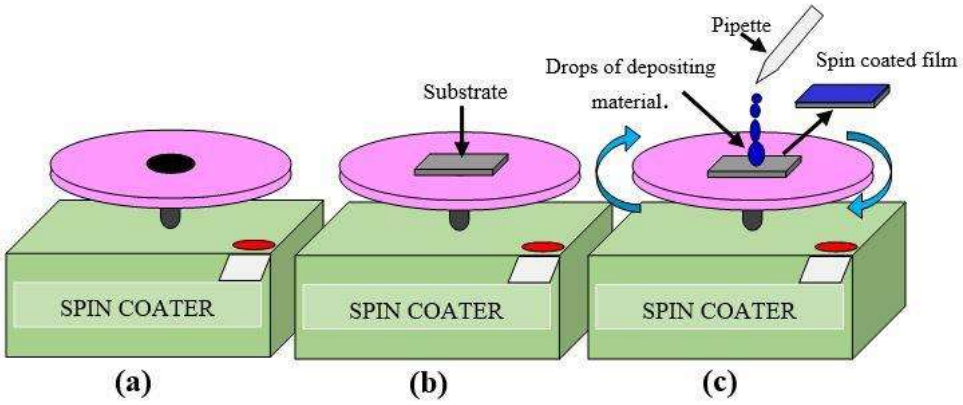

Figure 1.7: Spin-coating process steps (a) Spin coating unit (b) Sample loaded on the spin coating unit and (c) Coating on the sample and sample with the spin-coated film.

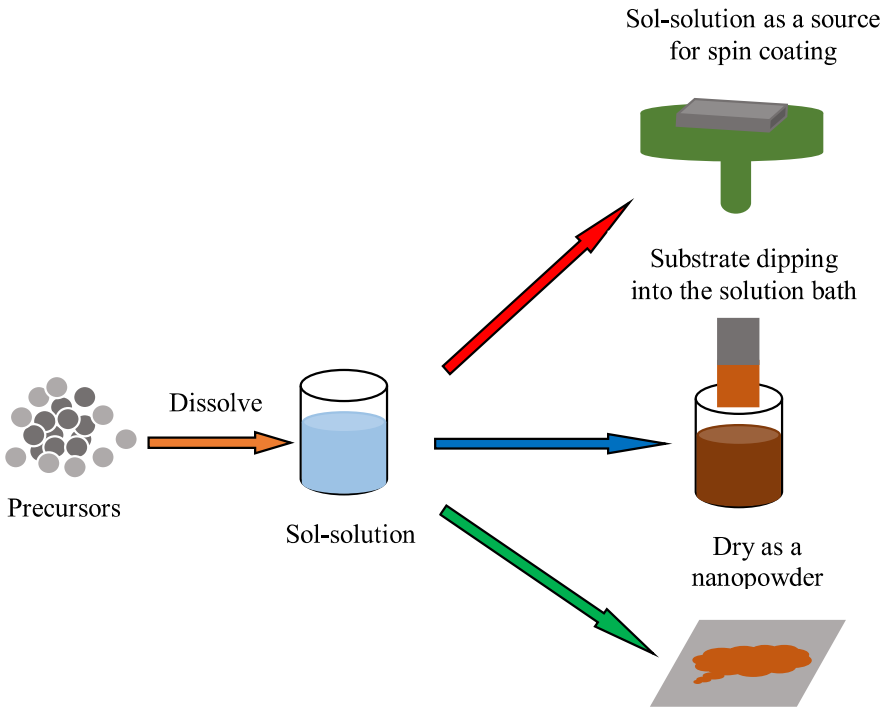

Figure 1.8: Sol-gel process.

1.4 Characterization Techniques for Thin Films and Devices

The deposited TF metal oxide and the fabricated TF devices are characterized using several techniques (instruments). The properties like surface morphology, roughness, surface structures, molecular orientation, etc., have a dominant role in the performance of the TF devices. Therefore, the TF is analyzed before the fabrication of the TF device; and finally, TF devices are analyzed for electronic and sensing properties. This section includes a brief discussion on the characterization tools used in the present thesis work.

1.4.1 Atomic Force Microscopy

Atomic force microscopy (AFM) is commonly used to imagine, measure, and manipulate matter at the nanoscale level. AFM gathered the information through "feeling" or "touching" the surface using a mechanical probe connected to the cantilever. The basic block diagram of the AFM and its operation is shown in Figure 1.9.

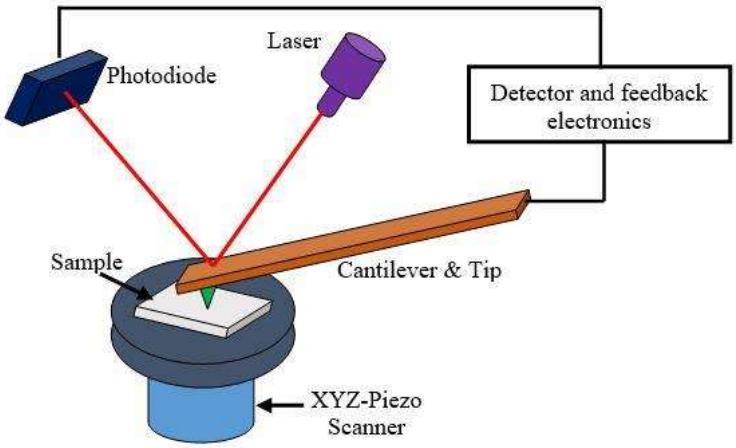

Figure 1.9: Working process of AFM.

The cantilever gets deflected by the sample's surface due to the interatomic force between the sample surface and the probe tip. The cantilever's deflection is measured by the in situ laser light [Hameed *et al*. (2018)]. Various properties such as the thickness, surface height, roughness, magnetism, etc., of the nanostructured materials can be extracted from the AFM image [Seshan (2012)]. AFM is operated under three modes: static contact, dynamic non-contact, and dynamic contact or tapping.

1.4.2 Scanning Electron Microscopy

Scanning electron microscopy (SEM) is a focused electron beam based technique to investigate the surface characteristics, namely morphology, topography, and composition. In SEM, the fine beam's interaction to the surface emits secondary and back-scattered primary electrons. The basic operation of SEM with a schematic representation is shown in Figure 1.10.

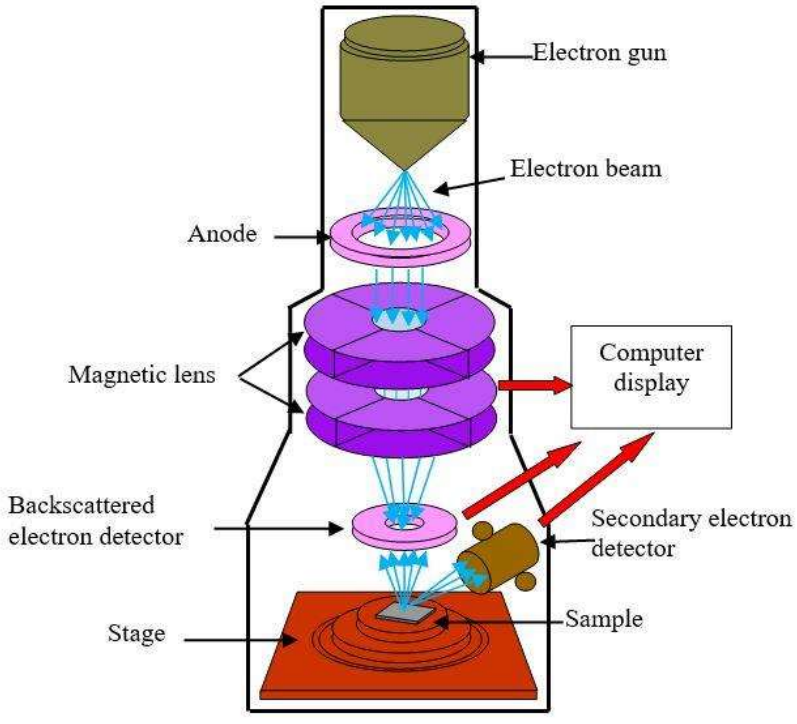

Figure 1.10: Working diagram of SEM.

The emitted electrons are collected and amplified to create an image on a computer display corresponding to the surface topography [Webb and Holgate (2003)]. The samples' elemental identification and quantitative composition are measured using the in-built energy dispersive X-ray analyzer (EDX or EDA) of the SEM system.

1.4.3 X-Ray Diffraction

X-Ray diffraction (XRD) is used to find out the information regarding the crystal phase, the lattice constant, and the average particle size. In this method, an X-ray beam incident on the surface of the sample to interact with the material in a non-destructive manner [Schroder (2006)]. When X-rays are penetrated inside any material/matter, the uniform spacing of atoms in the material/matter produces an interference pattern due to the diffraction phenomenon. The Bragg equation defines the resolution of the XRD pattern ($n\lambda=2d\sin\theta$), where n, λ, d, and θ are an integer, wavelength of the X-ray, the interplanar spacing, and the angle of the X-ray beams, respectively [Nasrollahzadeh *et al*. (2019)]. The operation of XRD is illustrated in Figure 1.11.

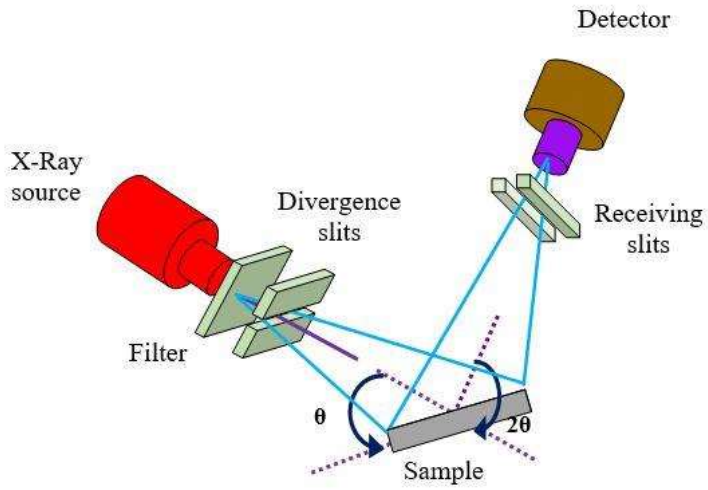

Figure 1.11: Working process of XRD.

1.4.4 Electrical Characterization Techniques

The electrical characterization is performed to extract various parameters related to conductivity, device, and sensor performance. The change in charge carrier concentration or conductivity under the applied voltage is the critical electrical quantity measured for the device parameter calculated using a semiconductor parameter analyzer. Also, the change in electrical parameters of the device under the exposure of gases is measured to calculate various gas sensor parameters. The electrical measurement techniques employed in the thesis work are briefly described as follows.

The change in the current flowing through the device for the change in the applied bias voltage is characterized by current-voltage (*I-V*) [Sze. (1981)]. The *I-V* measurements have been used to calculate the gas response (sensitivity), response-recovery time, and selectivity of the fabricated MSM based gas sensor. The variation in the junction capacitance for the applied bias voltage across the junction is characterized by capacitance-voltage (*C-V*) [Sze (1981)]. The *C-V* measurements have been used to calculate the gas response (sensitivity), response-recovery time, and selectivity of the fabricated MOS capacitor-based gas sensor. The gas sensing measurement is performed by placing the fabricated gas sensors inside a homemade self-design gas sensing chamber of 10-liter water volume capacity with gas inlet and outlet valves facilities, as shown in Figure 1.12. A mass flow controller (MFC) is provisioned at the gas sensing chamber inlet to inject the gas inside the chamber. If 100 ml of gas is injected inside the chamber, then it represents the 1% concentration of gas (in 10 liters of the chamber). A heating chuck at the bottom inside the chamber works as a base for the probing using a magnetic micro-positioner to hold the sample. A fan is also used inside the chamber for uniform distribution of the gas.

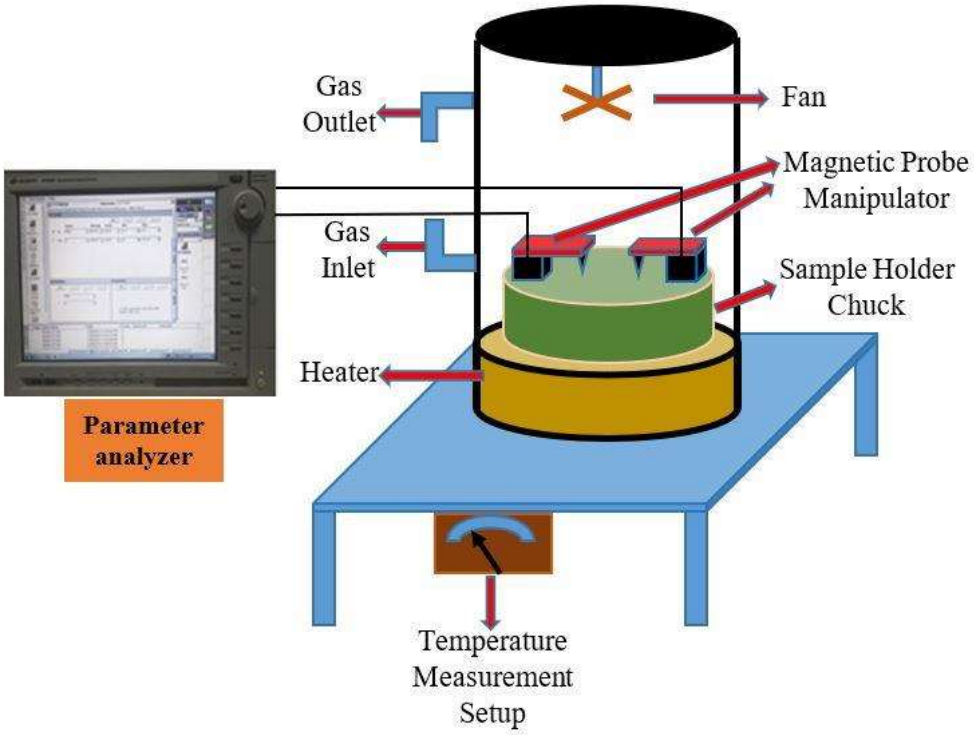

Figure 1.12: Block diagram of the gas sensing chamber.

1.5 Literature Review

The present thesis's objective is to examine the gas sensing properties of some TiO_2 TFs and Colloidal ZnO QDs TFs based hydrogen sensors with emphasis on room-temperature performance**.** Some critical literature on metal oxides based gas sensors for hydrogen detection is reviewed in the subsequent sub-sections to outline the scope of the thesis.

1.5.1 Review of TiO_2 Based Hydrogen Sensors

The metal oxides have the benefits of low-cost processing, easily available, and environment friendly. Although most of the metal oxides are sensitive to hydrogen gas, TiO_2 is more appropriate for hydrogen gas sensing due to biocompatibility and abundance in nature [Luo *et al.* (2017)]. One of the earliest works on the TiO_2 based gas sensor was reported by Yamamoto et al. using a Schottky diode structure in 1980 [Yamamoto *et al.* (1980)]. Schottky diode fabricated in Pd/TiO_2 structure has more

sensitivity towards hydrogen than Pt/TiO_2 and Au/TiO_2 structures. The gas response was selective and quantitative to monitor the hydrogen in the air at the fixed applied voltage. However, gas response, rise time, and fall time have been enhanced at a higher operating temperature. The comparative studies on gas sensing abilities of Pt/TiO_2 and Pt/SnO_2 based Schottky barriers were reported by Schierbaum *et al.* in 1991. The gas-sensing performance was improved by metal/oxide interface engineering and adjusting the dopant distribution. Hayakawa *et al.* (2000) fabricated a platinum dispersed-TiO_2 thin film-based sensor with high selectivity and sensitivity of 60% for 1000 ppm of H_2 at 200°C. Du. *et al.* (2002) developed a TiO_2/PtO-Pt dual layer-based resistive hydrogen sensor and observed the sensitivity of 75% at 200°C.

Later, Yadava. *et al.* reported the capacitive hydrogen sensor using thermally deposited TiO_2 in 2007. A maximum gas response of 54% was found for a hydrogen concentration of 8% in the N_2 atmosphere at room temperature. The thick film deposition technique by the screen-printing method was used by Zhang *et al.* in 2010 to fabricate a 30 μm thick TiO_2 sensing layer on Al_2O_3 substrate. The shortest response-recovery time was found when the sensor was annealed at 900°C for two hours. The Pt and Pd embedded anodic TiO_2 nanotube (NT)-based resistive hydrogen sensor was developed by Joo *et al.* in 2010 that was operated at 290°C. Esfandiar *et al.* fabricated the sol-gel coated TiO_2 based composite with chemically reduced graphene oxide in 2012 and achieved a decent gas response for the 100-1000 ppm of hydrogen at 180°C.

Further, Pd functionalized nanocrystalline TiO_2 thin film-based resistive sensor was fabricated by Kanungo *et al.* in 2015 and obtained a maximum sensitivity of 78% at 120°C for 1% of hydrogen gas. It is also found that the structural modification of TiO_2 largely enhanced the sensitivity. The Pd decorated tubular TiO_2 thin film was obtained

using anodization by Moon *et al.* in 2016. The obtained sensitivity was in the range of 1.25-7800 for 10-5050 ppm H_2 and 25-17000 for 10-1000 ppm H_2 in synthetic air and N_2 atmosphere, respectively, at the operating temperature range 140-180°C. The effect of the porous Pd film on the TiO_2 nanorods (NRs) was investigated by Erdem *et al.* for H_2 detection in 2016. The observed gas response was low at 30°C, but the improved response-recovery, stability, and reproducibility were achieved at a higher temperature (~200°C). In another work reported by Chen *et al.* (2016), a porous nanocomposite of Pt and TiO_2 based MSM hydrogen sensor resulted in the sensitivity of 10000 for 1000 ppm of H_2 in a nitrogen environment at room temperature.

1.5.2 Review of ZnO Based Hydrogen Sensors

ZnO based gas sensors have shown reliable, repeatable, and stable sensing performance for various gases such as H_2, nitrogen dioxide (NO_2), methane (CH_4), carbon dioxide (CO_2), hydrogen sulfide (H_2S), ammonia (NH_3), and volatile organic compounds (VOCs) [Zhang *et al.* (2010), Forleo *et al.* (2010), Ra *et al.* (2010), Ranwa *et al.* (2016)]. ZnO based gas sensors have advantages of lower-cost, easier synthesis technique, bio-compatible, and environment friendly nature [Wang *et at.* (2006), Law and Thong (2008), M. Kumar *et al.* (2017)].

One of the earliest works on the ZnO-based gas sensor was carried out by Bott *et al.* in 1984. The gas sensor was fabricated on ZnO single crystals and found that the sensor was sensitive to carbon monoxide and hydrogen but insensitive to methane and water vapor. The sensor is also shown to have long-term stability with a response time of ~120 s when operated at a temperature above 390°C. In the year 1989, Egashira *et al.* detected that the responses of Li^+-doped ZnO are larger than the undoped ZnO whiskers for 1% H_2 in the temperature range of 200°C to 700°C. Later, a systematic investigation

of the electrical conductivity and gas sensing performance of ZnO thin films obtained via spray pyrolysis was carried out under the presence of uniformly distributed Pt as a catalyst by Pizzini *et al.* (1989) for the temperature dependence in the temperature range of 498-573 K. Pure ZnO, when sintered at 870 K have shown good response to hydrogen and ethanol, whereas it has shown good response for carbon monoxide when the small amount of copper as a catalyst is mixed and operated 650 K [Raju and Rao (1991)].

Further, in the year 2000, Xu *et al.* observed that sensitivity and selectivity could be enhanced by using noble metal with ZnO thin film. The comparative gas response for H_2 in the Pt-coated single ZnO nanorods and ZnO thin film of different thicknesses (20-350 nm) was investigated by Tien. *et al.* in the year 2005. Three times larger response is observed in Pt-coated single ZnO nanorods than thin films of ZnO for 500 ppm concentration of H_2 in an N_2 environment at room temperature. It is also found that deposition techniques have a leading role in gas sensing. Sadek. *et al.* (2007) used RF-sputtered single-crystalline ZnO nanobelts to achieve a gas response of 14.3 for 1% of H_2 at 385°C. In another work, Pandis *et al.* (2007) fabricated the Schottky contact between Au nanoclusters and pulsed laser deposited ZnO thin film on Si/SiO_2 substrate for hydrogen sensor operated at low-temperature. The fabricated sensors have shown a gas response of 45% for 3% H_2 at a lower temperature of 90°C. In the year 2009, Tamaekong *et al.* made a thick film (10 μm) of ZnO using the flame spray pyrolysis method for hydrogen sensors. The H_2 response is increased with increasing the Pt doping and sensor temperature, but the response was relatively lower.

Furthermore, the MEMS-based sensors using ZnO nanoflakes have been reported by Bhattacharya *et al.* in 2013 and got a response of ~80.7% for 2% of H_2 at ~150°C.

The composite of ZnO and SnO_2 was investigated by Mondal *et al.* for H_2 sensing and achieved a response of 90% for 1% of H_2 at 150°C in 2014. In 2015, Giancaterini *et al.* reported the ZnO-Pt-based sensor to measure a gas response of 23.80 at 1000 ppm H_2 and temperature at 300°C. Rajan *et al.* measured a gas response of 57% for 1000 ppm H_2 at 350°C in RF sputtered ZnO/Pt based Schottky diode grown on n-Si substrates in the year 2016. Later, Hassan *et al.* (2016) fabricated a ZnO thin film-based H_2 sensor using a bimetallic structure made of platinum/palladium (Pt/Pd) thin film and observed sensitivity of 13.56% for H_2 concentration 10,000 ppm (1 vol.%) at 150°C. Hassan and Chung (2017) reported a hydrogen response of 58% for 1% H_2 at 100°C in a Pt/Pd-decorated ZnO nanorod (NR) clusters based hydrogen sensor. Rajan *et al.* also fabricated the Pd/ZnO Schottky diode for hydrogen sensing in the same year and achieved the sensitivity of 224% at 150°C for 50 ppm of hydrogen gas. Lakshmanan *et al.* explored microwave-assisted ZnO nanospheres for H_2 sensing and measured a gas response of 39% at 2% of H_2 at room temperature (27°C), reported in 2018. Continuous efforts are being made by the researchers to improve the sensitivity and selectivity of the ZnO nanostructure-based gas sensors [Huh *et al.* (2011), Abubakar *et al.* (2017)].

1.5.3 Major Observation from the Literature Survey

In this section, the major observations derived from the literature survey on the TiO_2 and ZnO based gas sensor are summarised as given in the following:

- Hydrogen (H_2) gas is projected as one of the best alternative fuels for the future due to the limited stock of fossil fuels in nature.
- The major difficulties in storing and exporting H_2 are associated with its extremely inflammable nature, which may cause an explosion at even a 4% limit in the atmosphere.

- ❖ TiO_2 and ZnO are the most widely used metal oxide semiconductors for gas sensing applications due to their lower-cost, easier synthesis techniques, and environmentally friendly nature.
- ❖ Sensors fabricated using thin-film nanostructures of TiO_2 and ZnO have the capability to operate at a lower temperature compared to the sensor fabricated using thick film.
- ❖ The sensitivity of hydrogen sensors fabricated by TiO_2 and ZnO nanostructures can be increased by using noble metal as electrodes. Higher sensitivity is obtained at higher operating temperatures.
- ❖ Although various ZnO nanostructures have been explored for hydrogen sensing applications, but colloidal ZnO quantum dots have not been reported for hydrogen sensing applications.
- ❖ There is a high demand for sensitive, low-cost, reliable, and accurate H_2 gas sensors to monitor any leakage of hydrogen during its production, transportation, and storage at low temperatures.

1.5.4 Challenges in Metal Oxide Based Hydrogen Sensors

The metal oxide-based sensors are capable of sensing the hydrogen gas, but most of the hydrogen sensors are generally operated at a higher temperature. The high temperature of operation of the sensor may result in fire due to the explosive and flammable nature of hydrogen. So, there is always a challenge to fabricate a sensor that can be operated at a lower temperature or room temperature. Hydrogen sensors are mostly based on the change in resistance and faced a critical issue with sensor stability. The low gas response towards the small concentration of hydrogen is also another issue. Therefore, the fabrication of desired hydrogen sensors that meet the essential and

logical requirements such as small size, room temperature operability, high gas response, fast response/recovery time, and mass production with minimal cost and less circuit complexity are the major challenges in the field of hydrogen sensor. The metal oxide-based hydrogen sensor should be optimized for the selective towards hydrogen since metal oxides are also sensitive to many gases and organic vapours. A similar change in resistance took place with an n-type CNT-based hydrogen sensor. It should be noted that fiber optic localized surface plasmon resonance (LSPR) hydrogen sensor also works on the adsorption mechanism. The nanomaterial chemically or physically adsorbs the gas molecules in the fiber optics. The optical properties are modulated due to the adsorption of hydrogen gas, and the gas response is evaluated from the change in optical parameters of the fiber optics.

Thus, metal oxide-based electronic sensors performance and working capability are similar to the CNT and fiber optic LSPR based sensors. But, the metal oxide-based electronic sensor has the advantage of the low-cost fabrication and measurement.

1.6 Motivation and Problem Definition

Mostly hydrogen sensors are fabricated in either resistive or capacitive structures and operated at higher working temperatures. For the resistive hydrogen, various structures such as resistors, metal-semiconductor-metal (MSM), diodes, heterostructures, and transistors are investigated. The capacitive sensor using metal oxide semiconductor (MOS) structure is preferred over these resistive sensors due to relatively stable response and low energy consumption. In view of the above, the objective of the present thesis is to fabricate the nanoparticle/quantum dots based TiO_2/ZnO TFs that can enhance gas response for hydrogen. Thin-film engineering using advanced deposition techniques can improve the sensitivity of the TiO_2/ZnO based gas sensor. The optimized

film thickness of TiO_2/ZnO film may lead to enhance the gas response and reduce the cost of the sensor. Thin-film deposition techniques such as thermal deposition, electron beam evaporation (EBE), and spin-coating can be employed for better electronic and sensing properties.

1.7 Scopes of the Thesis

The present thesis deals with the fabrication and characterization of some TiO_2 thin films and colloidal ZnO quantum dots-based hydrogen sensors with emphasis on room-temperature operations. The thesis consists of SIX chapters, including the present one. The contents of the remaining FIVE chapters are briefly described in the following:

Chapter-2 deals with the investigation of electrical and hydrogen sensing properties of sol-gel derived TiO_2 film-based metal-semiconductor-metal (MSM) structure with an interdigitated electrode. The TiO_2 active layer is deposited on a SiO_2 coated Si substrate by the low-cost spin coating method where the SiO_2 layer is grown by thermal oxidation of the Si substrate. The change in current is measured for different concentrations of H_2 gas at room temperature and 175°C in an ambient air atmosphere. Gas responses of 7.93%, 13.14%, 18.62%, and 26.75% for 1% H_2, 2% H_2, 3% H_2, and 4% H_2 gas are obtained respectively in ambient air condition at 175°C while no significant response is observed at room temperature. Sensors made using TiO_2 have shown high stability and repeatability in the ambient environment and identical conditions. The objective of this study is to demonstrate the non-suitability of the sol-gel derived TiO_2 film and metal-semiconductor-metal structured device for room-temperature hydrogen sensing applications.

Chapter-3 investigates the room-temperature hydrogen sensing properties of the thermally evaporated TiO_2 films. The proposed device was a Pd/TiO_2/Si/Al structure-

based metal oxide semiconductor (MOS) sensor. Top circular Pd metal contact is used as gate whereas bottom Al contact to the p-type silicon (Si) substrate is used as bulk contact. The proposed MOS sensor is characterized by capacitance-voltage (*C-V)* and conductance-voltage (*G-V)* measurements under exposure of different concentrations of H_2 gas at room temperature in the ambient-air atmosphere. The maximum gas response of 65% was calculated from the change in capacitance and 84% was calculated from the change in conductance at 4% of H_2 gas. The obtained maximum gas responses obtained from two different measurement techniques confirm the detection possibility of low concentration of hydrogen gas (4%) of our fabricated MOS sensor operated at room temperature under zero bias voltage conditions.

Chapter-4 deals with the investigation of the hydrogen sensing property of TiO_2 thin films fabricated by the electron beam (e-beam) evaporation (EBE) method. The device structure considered for the present study was the MOS sensor considered in Chapter-3. The MOS sensor is fabricated by depositing the e-beam evaporated TiO_2 film on the Si substrates oxide followed by the deposition of a thermally evaporated palladium (Pd) electrode on the active layer of the sensor. The response of the MOS sensor for H_2 gas is measured in the form of a shift in capacitance-voltage (*C-V*) and conductance-voltage (*G-V*) characteristics. The maximum sensitivities for 4% H_2 gas are found as 84% and 90% in ambient air and nitrogen gas, respectively. The fabricated $Pd/TiO_2/Si$ MOS sensor shows fast response and recovery for H_2 gas. The selectivity of the MOS sensor with most interfering organic vapors such as acetone, chloroform, ethanol, isopropanol, and methanol are also investigated.

Chapter-5 investigates the hydrogen sensing properties of colloidal ZnO quantum dots based MSM structure with interdigitated electrodes. The active layer is obtained by

spin coating of as-synthesized colloidal ZnO QDs on the SiO_2 coated Si substrate where the SiO_2 layer is grown by oxidation of the Si substrate. The change in current is measured for different concentrations of H_2 gas at 175°C in an ambient air atmosphere. Reasonably good gas responses of ~41% for 1% H_2 gas and 83.2% for 4% H_2 gas have been obtained in ambient air conditions. High selectivity of the proposed sensor with respect to ammonia, sulfur dioxide, and organic vapors such as acetone, methanol, chlorobenzene, and chloroform have also been achieved. In this case we also fabricate the set of 10 device and sensors made using ZnO QDs have shown high stability and repeatability in the ambient environment and identical conditions.

Finally, **Chapter-6** summarizes the major observations and concludes the major findings of the present thesis. This chapter also outlines some future scope of works related to this thesis.